frontiers | Frontiers in Environmental Chemistry

TYPE Original Research
PUBLISHED 13 June 2024
DOI 10.3389/fenvc.2024.1416702

OPEN ACCESS

EDITED BY
Zhen Wei,
Beijing University of Technology, China

REVIEWED BY
Meili Liu,
University of Miami, United States
Kefeng Shang,
Dalian University of Technology, China

*CORRESPONDENCE
Ester Marotta,
ester.marotta@unipd.it

RECEIVED 12 April 2024
ACCEPTED 16 May 2024
PUBLISHED 13 June 2024

CITATION
Giardina A, Lofrano G, Libralato G, Siciliano A, Marotta E and Paradisi C (2024), Air non-thermal plasma, a green approach for the treatment of contaminated water: the case of sulfamethoxazole.
Front. Environ. Chem. 5:1416702.
doi: 10.3389/fenvc.2024.1416702

Air non-thermal plasma, a green approach for the treatment of contaminated water: the case of sulfamethoxazole

Agata Giardina[1], Giusy Lofrano[2], Giovanni Libralato[3], Antonietta Siciliano[3], Ester Marotta[1]* and Cristina Paradisi[1]

[1]Department of Chemical Sciences, University of Padova, Padova, Italy, [2]Department of Movement, Human and Health Sciences, University of Rome "Foro Italico", Rome, Italy, [3]Department of Biology, University of Naples Federico II, Naples, Italy

Non-thermal plasma (NTP) is gaining increasing attention as a promising approach for advanced water treatment to degrade persistent organic pollutants. Aqueous solutions of sulfamethoxazole (4-amino-N-(5-methylisoxazol-3-yl)-benzensulfonamide, SMZ), an antibiotic largely employed for humans and animals and a widespread persistent pollutant of waters and wastewaters, were subjected to air NTP treatment in a dielectric barrier discharge (DBD) reactor. The effects of SMZ initial concentration and of the solution pH on SMZ decomposition kinetics and transformation products were investigated. Efficient degradation was achieved, resulting in the complete removal of SMZ (10 μM initial concentration) in less than 25 min treatments, in the exhaustive mineralization (a result never reported before in plasma treatments and seldom reached also with other advanced oxidation processes) of all organic carbon in 6 h and in an energy efficiency of 6.4 g/kWh at 50% conversion. By means of HPLC-UV/Vis and LC-ESI-MS^n analyses, a number of organic transformation products was identified along the path to SMZ mineralization, all present always in very small amounts and in turn decomposed at short treatment times. The effect of the solution pH on the genesis and decay of transformation products was also investigated. Based on comparisons with literature data and on previous findings obtained with the DBD reactor used in this work, it is concluded that the major reactive species involved in the degradation of SMZ are the hydroxyl radical and ozone. Finally, toxicological analyses of water initially containing 0.5 mM SMZ and subjected to 4 h NTP treatment showed that the by-products are not toxic to *Raphidocelis subcapitata* and *Daphnia magna*, while residual toxicity was detected by *Aliivibrio fischeri*.

KEYWORDS

atmospheric plasma, water treatment, antibiotics, ozone, hydroxyl radical, complete mineralization

1 Introduction

Increasing demand for clean water resources and concerns for environmental pollution by persistent chemicals are promoting the search for novel approaches to achieve better performance than presently available in water decontamination treatments (Oberoi et al., 2019; Qiao and Xiong, 2021; Ang et a., 2022; Subramaniam et al., 2022; Naghdi et al., 2023). Among the novel solutions being considered for AOP (Advanced Oxidation Process) based

stages, most appealing are those applying electric discharges to produce highly reactive cold plasmas (also called non-thermal plasmas, NTP) within or in contact with the polluted water. Thus, the production of NTP and its application to water treatment do not require heat, vacuum or pressure, additives or catalysts, but need only electricity (Jiang et al., 2014; Foster, 2017; Shang et al., 2019; Takeuchi and Yasuoka, 2021; Aggelopoulos, 2022). Coupled to a renewable source of energy, therefore, NTP-based approaches qualify as candidates for perspective new green water treatment technologies.

In most studies, non-thermal plasma is produced by the application of either dielectric barrier discharges (DBDs) or corona discharges in air at room temperature and atmospheric pressure. Such discharges bring about excitation, ionization and dissociation of gaseous molecules resulting in the emission of radiation and in the production of many reactive species (e.g., electrons, ions, atomic oxygen and hydrogen, OH radicals, ozone, hydrogen peroxide) within the gas phase in contact with the aqueous media (Bruggeman et al., 2016). These species can attack organic pollutants present in the water, either at the plasma/liquid interface or within the aqueous phase. Other approaches employ electrical discharges directly in the liquid and discharges in bubbles/vapor within the liquid (Vanraes et al., 2016; Bosi et al., 2017).

Due to the presence of both oxidizing and reducing reactive species, including, as mentioned above, electrons, ions, and OH radicals, non-thermal plasmas are extremely powerful and versatile tools to activate energy demanding chemical reactions. Specifically, NTPs are capable of initiating both advanced reduction and advanced oxidation processes (AROPs) (Tomei et al., 2023). Thus, NTP-based water treatments have been reported to degrade effectively not only the majority of recalcitrant organic pollutants, which react directly with OH radicals, but also important exceptions, like PFAS (per- and polyfluoroalkyl substances), which are not attacked by OH radicals but react instead with electrons (Biondo et al., 2023).

This paper reports on the application of air non-thermal plasma to degrade sulfamethoxazole, a widespread antibiotic and a quite persistent water contaminant. Pharmaceuticals form a major class of water organic contaminants, causing increasing concern for their potential toxic impact on the environment. Drugs often possess physicochemical properties that favour their presence and persistence in wastewater and surface water, such as polarity, significant hydrosolubility and high stability and half-life (Andreozzi et al., 2003). It is known that some of the substances detected can affect organisms in the environment. Although the health effects imputable to unintended chronic pharmaceutical exposure of humans and animals, as well as of ecological communities, are not yet fully identified and understood, they are raising global concern and challenge to find suitable remediation solutions. For this reason, the European Directives have included some of them in water watch lists and imposed their monitoring in drinking water (EU, 2022). Antibiotics are the most common pharmaceuticals detected in acquatic ecosystem. Due to their antimicrobial activity, they are hard to eliminate by means of conventional oxidation methods. Among various AOPs being presently pursued for the remediation of antibiotics-contaminated water and soil (Morin-Crini et al., 2022), NTP-based technology is viewed as a most promising perspective option (Magureanu et al., 2015; Magureanu et al., 2021).

The antibiotic sulfamethoxazole (4-amino-N-(5-methylisoxazol-3-yl)-benzensulfonamide, SMZ), the selected target for this study, was originally designed for humans but is presently sharing also a large fraction of the global market in animal food industry. Since natural degradation of SMZ by means of biological processes (Wang and Wang, 2018) is not very facile, great efforts are being spent in searching and developing alternative AOP based treatment stages. There is indeed a vast literature reporting on SMZ degradation pathways and efficiency in ozonation and many other AOPs (Prasannamedha and Senthil Kumar, 2020). Sulfamethoxazole is thus an excellent model to test the performance of NTP based degradative treatments of sulfamidic drugs in water. A very recent paper (Bilea et al., 2024) provides a critical account of most recent results obtained so far with different NTP-setups, including also integrated processes combining the effect of NTP with that of catalysts, like Ti/C-N-TiO_2 (Mouele et al., 2022) and MnO_2/Cellulose acetate (Zhang et al., 2022), or additives such as persulfate (Shang et al., 2022; Wang et al., 2022) peroxymonosulfate and peroxydisulfate (Shang et al., 2022). These and related studies show that NTP is in general quite effective in bringing about the degradation of SMZ, whereas mineralization, i.e., total conversion into inorganic products (carbon dioxide, sulfate, ammonium and nitrate ions) is way more difficult to achieve.

In this work we investigated the degradation of SMZ in aqueous solutions using a dielectric barrier discharge (DBD) reactor which generates NTP in the air above the liquid. DBDs are being widely used in research and applications because they can degrade organic pollutants in water under mild conditions, work under simple operating conditions, offer good discharge stability and high treatment efficiency and are easily coupled with catalysts (Guo et al., 2023; Hu et al., 2023). Our DBD reactor works at low power and can be operated for long treatment times maintaining stable and reproducible discharge conditions. It is thus most suitable for kinetic studies and for investigating slow processes like mineralization of refractory organic pollutants (Ceriani et al., 2018a; Giardina et al., 2019; Tampieri et al., 2019). Along the route to mineralization, many organic intermediate products (*transformation products*) are expected to form and in turn undergo NTP induced degradation. It is evident from the literature results reported above, that some of these transformation products are less reactive than their precursor, SMZ, and in the worst scenario, they might as well be as toxic or even more toxic than SMZ itself. One motivation for carrying out this study was, therefore, to verify the possibility of achieving 100% mineralization of SMZ in aqueous solution. On the other hand, an advanced water treatment stage is usually meant to achieve environmentally safe quality levels rather than a full mineralization. Therefore, we also carried out detailed product analyses and toxicity tests on SMZ solutions treated with plasma for way shorter times than required for mineralization and still containing considerable amounts of dissolved organic carbon. This major part of the study involved extensive product investigations performed by LC/MS and LC/MS/MS analyses and parallel toxicity tests carried out with *Daphnia magna*, *Vibrio fischeri* and *Raphidocaelis subcapitata* and standardized bioassays. The results obtained show the excellent reactivity of NTP, which succeeded in

achieving mineralization of a resistant sulfa drug like SMZ and confirmed its potential for development into a novel technology for advanced oxidation stages in water treatment. This work also underlines the powerful diagnostic capabilities of MS/MS analysis, sustained by preexistent knowledge and, most importantly, by the rational interpretation of the spectra, in detecting and characterizing transformation products including isomers.

2 Materials and methods

2.1 Materials

Sulfamethoxazole and H_3PO_4 (85 wt% in H_2O) were purchased from Sigma-Aldrich while KH_2PO_4 and $K_2HPO_4{\cdot}3H_2O$ from Carlo Erba. Ultrapure grade water (milliQ a Millipore system), obtained by filtration of distilled water with a Millipore system, was employed for all the experiments. Pure air used in the experiments was a synthetic mixture (80% nitrogen e 20% oxygen) from Air Liquid with specified impurities of H_2O (<3 ppm) and of C_nH_m (<0.5 ppm).

2.2 Experimental apparatus

The experimental apparatus employed in this work is a dielectric barrier discharge (DBD) reactor, employing a wire/plate electrode configuration, which was previously applied to the degradation of phenol (Marotta et al., 2011; Marotta et al., 2012), pharmaceuticals (Krishna et al., 2016; Madureira et al., 2017), pesticides (Giardina et al., 2018; Giardina et al., 2019), maleic and fumaric acids (Shapoval et al., 2023). The reactor is made of a glass vessel (i.d. = 95 × 75 mm, h = 60 mm) with a Teflon cover holding four passing stainless-steel electrodes. The electrodes support two parallel wires of 75 mm length and 0.15 mm diameter fixed upon their tips. The wires, made of stainless steel, are placed at a reciprocal distance of 38 mm and 15 mm above the aqueous solution. A volume of 70 mL of SMZ prepared solutions was employed in all the experiments, which corresponds to a thickness of 10 mm of liquid inside the reactor. The outer surface of the reactor base is covered with a film of silver and is electrically connected with the ground. The discharge is generated by an AC high voltage transformer with an effective voltage of 18 kV and a frequency of 50 Hz. For all the experiments the voltage was kept constant and voltage-current measurements were performed with a digital oscilloscope (TDS5032B, bandwidth 350 MHz, sample rate 5 G/s) to verify the reproducibility of the electrical conditions. A flow of air of 30 mL·min^{-1} was allowed through the reactor and the discharge occurred in the gas phase above the liquid surface. To minimize evaporation phenomena from the solution to be treated, the air was humidified by passing it through a water bubbler placed before the reactor. Control experiments assured that the concentration of sulfamethoxazole remains constant in the solution when the humidified air is flowing in the absence of the discharge.

2.3 Sulfamethoxazole treatment experiments

Aqueous sulfamethoxazole solutions (70 mL) were prepared in Milli-Q water and phosphate buffer at pH 2, 7 and 11 and were subjected to plasma treatment. For experiments carried out at fixed pH, aqueous solutions were buffered by the addition of suitable amounts of Na_2HPO_4, KH_2PO_4 and H_3PO_4, with a buffer concentration of $2{\cdot}10^{-2}$ M. The efficiency of the decomposition process was determined by measuring SMZ conversion as a function of treatment time. To this purpose, at desired reaction times, the discharge was interrupted and a 0.5 mL aliquot of the treated solution was withdrawn and analyzed by HPLC (Thermo Scientific Products instrument with P2000 pump and UV6000LP Diode array detector). A Phenomenex Kinetex C18 column (5 µm C18 100A, 150 × 4.6 mm) was used and a mobile phase composed of water with 0.1% of formic acid (eluent A) and acetonitrile with 0.1% of formic acid (eluent B). The LC gradient for the separation was: from 0 to 20 min, a linear increase of B from 5 to 100%. Then 2 min of isocratic elution and finally the initial conditions were re-established in 10 min. The elution was monitored by UV analysis at wavelengths of 270, 314, and 370 nm. The fraction of residual drug expressed as C/C_0, where C_0 and C are the initial concentration and the concentration after treatment time t, respectively, was plotted against treatment time t and the data were fitted by Eq. 2.1

$$C = C_0 \cdot e^{-kt} \tag{2.1}$$

to obtain k, the observed rate constant of the process.

The energy efficiency of the plasma process was expressed by G_{50}, defined as the mass of the pollutant degraded per kWh of energy needed to halve the initial concentration of the pollutant Eq. (2.2),

$$G_{50}\left(\frac{mg}{kWh}\right) = \frac{1.8 \cdot 10^9 \cdot C_0\left(\frac{mol}{L}\right) \cdot V\,(L) \cdot MM_{SMZ}\left(\frac{g}{mol}\right)}{P\,(W) \cdot t_{\frac{1}{2}}\,(s)} \tag{2.2}$$

where V is the treated volume of the solution, MM_{SMZ} is the molar mass of SMZ, P is the electrical power (2.6 W) and $t_{1/2}$ is the half-life time of SMZ calculated as ln (2)/k. P was measured by averaging the instantaneous power over an integer number of cycles of the power frequency. The voltage and current signals were recorded by the digital oscilloscope and processed off line using a program written in Matlab language. Further details on power measurement are given in Ceriani et al. (2018b).

The pH of the initial and of the plasma treated solutions was measured with a pH meter Seven Compact, S220 (Mettler Toledo).

The antibiotic decomposition products were identified through the analysis of selected samples by liquid chromatography (Agilent Technologies 1100 series) connected to a diode array and a mass spectrometer detector (MSD Trap SL model G2245D). The conditions (column, eluents, gradient) were the same as described above. The ionization was performed within an electrospray (ESI) source alternating positive and negative polarity with the following parameters: nebulizer 50 psi, dry gas flow rate 11 L/min, dry gas temperature 350°C. The assignment of the oxidation products was performed by comparison of their retention time, UV/Vis and MS spectra with those obtained from

standard compounds, when available. Otherwise, peaks were tentatively attributed to specific intermediate products based on MS/MS spectra and comparison with data reported in the literature.

The total carbon (TC) present in SMZ solutions before and after NTP treatment, was determined by a TOC analyzer (Shimadzu TOC-VCSN instrument). It operates in the range of 50 µg/L–25 g/L and is equipped with an autosampler and an automatic diluter. Calibration of the instrument was carried out by using solutions of standard potassium hydrogen phthalate automatically diluted in the range of interest.

2.4 Toxicity assessment

The toxicity tests were carried out on untreated (SMZ $5{\cdot}10^{-4}$ M) and treated (after 4 h of non-thermal plasma) solutions. Negative controls were carried out on ultrapure water. Toxicity was investigated in accordance to Lofrano et al. (2016) via a battery of acute (A) and chronic (C) toxicity tests including biological models belonging to various trophic levels like *Aliivibrio fischeri* (A), *Raphidocelis subcapitata* (C) and *Daphnia magna* (A).

Toxicity tests with *A. fischeri* (NRRL-B-11177) were carried out according to ISO (1998). The luminescence was measured with a Microtox® analyzer (Model 500, AZUR Environmental) after 30 min at 15°C. Tests were carried out in triplicate. Data were analysed with Microtox Omni® software and the result expressed as percentage of bioluminescence inhibition (%).

Microalgae growth inhibition test with *R. subcapitata* was carried out according to ISO (2012). Cultures were kept in Erlenmeyer flasks. The initial inoculum contained 10^4 cells mL^{-1}. The specific growth inhibition rate was calculated considering six replicates exposed at (20 ± 1)°C for 72 h under continuous illumination (6000 lx). Effect data were expressed as percentage of growth inhibition.

Toxicity tests with *D. magna* were carried out according to ISO (2013). Newborn daphnids (<24 h old) were exposed in four replicates for 24 and 48 h at 20°C ± 1°C under continuous illumination (1000 lx). Before starting the test, they were fed with *R. subcapitata* (300,000 cells mL^{-1}) *ad libitum*. Toxicity was expressed as the percentage of dead organism.

All toxicity tests included the assessment of negative and positive controls in accordance with the specific reference method.

Toxicity was expressed as percentage of effect or as effective median concentration causing the 50% effect (EC50) on the exposed population. After the verification of homoschedasticity (F test, $p < 0.05$) and normality (Shapiro-Wilk test, $p < 0.05$) of toxicity data, the significance of differences between average values of different experimental treatments and controls was assessed by the analysis of variance (ANOVA, $p < 0.05$). When ANOVA revealed significant differences among treatments, *post hoc* tests were carried out with Tukey's test ($p < 0.05$). Statistical analyses were performed using Microsoft® Excel 2013/XLSTAT©-Pro (Version 7.2, 2003, Addinsoft, Inc., Brooklyn, NY, United States).

Toxicity data have been integrated according to Persoone et al. (2003) approach for natural water. According to Libralato et al. (2010), the hazard classification system based on percentage of effect (PE) includes a Class I for PE < 20% (score 0), Class II for 20% ≤ PE < 50% (score 1), Class III for 50% ≤ PE < 100% (score 2), Class IV when PE = 100% in at least one test (score 3) and a Class V when PE = 100% in all bioassays (score 4). Finally, the integrated class weight score was determined by averaging the values corresponding to each microbiotest class normalised to the most sensitive organism (highest score).

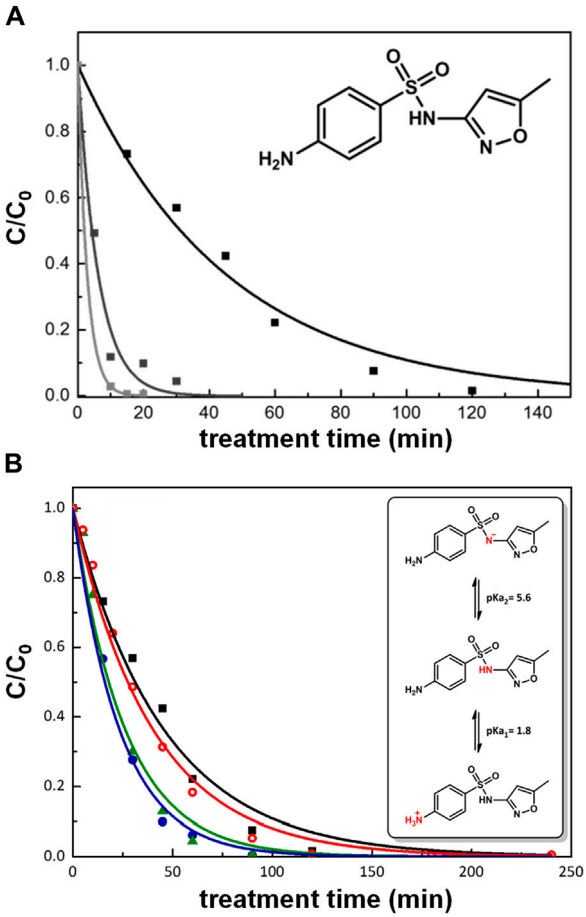

FIGURE 1
(A) Decay curves of SMZ treated at the following initial concentrations: $5{\cdot}10^{-4}$ M (black), $5{\cdot}10^{-5}$ M (dark grey) and $1{\cdot}10^{-5}$ M (light grey) and **(B)** at $C_0 = 5{\cdot}10^{-4}$ M under different pH conditions. (■) milliQ water; (○) buffer at pH = 2; (▲) buffer at pH = 7; (●) buffer at pH = 11.

3 Results and discussion

3.1 Efficiency of SMZ degradation: effects of initial concentration and of the solution pH

From the kinetic perspective, it was of interest to investigate the effects on SMZ degradation rate due to two important experimental variables, SMZ initial concentration and the solution pH. These experiments were all carried out at constant power.

SMZ solutions in milliQ water at three different initial concentrations (C_0), namely, $5{\cdot}10^{-4}$, $5{\cdot}10^{-5}$ and $1{\cdot}10^{-5}$ M, were treated in the DBD plasma reactor maintaining a constant power of 2.6 W. The degradation process was monitored by measuring the SMZ residual concentration (C) as a function of treatment time.

TABLE 1 Kinetic data for decomposition of SMZ in Milli-Q water, treated at different initial concentrations (C_0).

C_0 (M)	$k{\cdot}10^2$ (min^{-1})	$t_{1/2}$ (min)
$5{\cdot}10^{-4}$	2.2 ± 0.1	31
$5{\cdot}10^{-5}$	16 ± 2	4
$1{\cdot}10^{-5}$	35 ± 2	2

TABLE 2 Removal efficiency of SMZ ($C_0 = 5{\cdot}10^{-4}$ M) under different pH conditions.

Conditions	$k{\cdot}10^2$ (min^{-1})	$t_{1/2}$ (min)
Ultrapure water	2.2 ± 0.1	31
Buffer pH = 2	2.5 ± 0.1	28
Buffer pH = 7	3.8 ± 0.3	18
Buffer pH = 11	4.3 ± 0.2	16

Figure 1A shows the experimental results and the degradation curves obtained by interpolating the data with a first order exponential function, which provided values for the process rate constant (Table 1).

It is evident that the rate of SMZ decomposition depends on its initial concentration, C_0, the lower C_0 the faster its degradation. This phenomenon has been observed in many previous studies of NTP-promoted degradation of organic compounds in water (Madureira et al., 2017; Magureanu et al., 2021) including SMZ (Hu et al., 2023; Bilea et al., 2024), and attributed to competing reactions of the pollutant intermediate products with the reactive species generated by the discharge. A simple kinetic model accounting for these phenomena is described in the literature (Tomei et al., 2023 and references therein).

Since SMZ has acid/base properties, as detailed below, and the production and quenching of plasma-derived reactive species also depend on the solution pH, it was of interest to study the influence of pH on the degradation rate of SMZ in our reactor. Experiments were thus carried out under different pH conditions (pH 2, 7 and 11) using buffered aqueous solutions. Buffering is important because exposure to air plasma significantly affects the pH of water. A control experiment showed indeed that in the absence of a buffering system, the pH of 70 mL of pure milliQ water changed from neutrality to 2.8 during 240 min of plasma treatment in the reactor used here. Previous studies had demonstrated that this phenomenon is caused by the production of nitric acid, as a result of aqueous reactions of NOx formed by the discharge in the air above the treated water (Marotta et al., 2012). Moreover, in the presence of dissolved organic pollutants, changes in the solution pH are also due to the production of many organic acids intermediates along the path to complete mineralization, such as those found previously in the remediation of phenol in the same reactor as used here, including maleic, fumaric, muconic, oxalic, acetic and formic acids (Ceriani et al., 2018a). Figure 1B shows the degradation profile of SMZ (initial concentration $5{\cdot}10^{-4}$ M) observed in solutions buffered at pH 2, 7 and 11. It is seen (Figure 1B) that in all cases the experimental data fit reasonably well an exponential decay and that the decomposition rate depends on pH, the observed rate constant decreasing in the order k (pH 11) > k (pH 7) > k (pH 2) (Table 2).

In discussing these results, one should bear in mind that SMZ has acid/base properties and that the distribution of reactive oxidants generated in solution by plasma is also affected by pH. Thus, the observed effects can be attributed to two possible contributions, both pH-dependent, due, respectively, to the SMZ species and to the plasma-generated reactive oxidants which are prevailing in solution under the specific pH conditions tested. It is interesting to analyze these two contributions and attempt to estimate their relative importance. Depending on the solution pH, sulfamethoxazole partitions among three different species, anionic, neutral and cationic, as shown in the inset of Figure 1B, according to the following acid/base equilibrium constants: pK_{a1} = 1.8 and pK_{a2} = 5.6. In very acidic aqueous solutions the protonated form is predominant, with protonation occurring at the primary amino group on the benzene ring (Manzo and de Bertorello, 1973). At neutral pH, SMZ is largely deprotonated at the sulfanilamidic nitrogen as shown in Figure 1B. At pH 11, at which the maximum efficiency is observed, SMZ is completely deprotonated (Manzo and de Bertorello, 1973).

It was shown in previous studies conducted with the same plasma reactor as used here that ozone and hydroxyl radicals are the main reactive species involved in the oxidation of organic pollutants (Marotta et al., 2011; Krishna et al., 2016; Shapoval et al., 2023; Tomei et al., 2023). In this setup, OH radicals can be generated directly within the plasma in humid air via reaction of water with atomic oxygen (Eq. 3.1) and via electron induced dissociation of water (Eq. 3.2) (Marotta et al., 2008) as well as indirectly via decomposition of ozone in water (3.3–3.8), a process which is favored under basic pH conditions (Eqs 3.3, 3.4) (Staehelin and Hoigné, 1982; Shapoval et al., 2023; Tomei et al., 2023).

$$O(^1D) + H_2O \rightarrow 2^{\bullet}OH \quad (3.1)$$

$$H_2O + e^- \rightarrow {}^{\bullet}OH + {}^{\bullet}H \quad (3.2)$$

$$O_3 + {}^-OH \rightarrow O_2^{-\bullet} + HO_2^{\bullet} \quad (3.3)$$

$$O_3 + HO_2^{\bullet} \rightarrow 2\,O_2 + {}^{\bullet}OH \quad (3.4)$$

$$O_3 + {}^{\bullet}OH \rightarrow O_2 + HO_2^{\bullet} \quad (3.5)$$

$$O_3 + O_2^{-\bullet} \rightarrow O_3^{-\bullet} + O_2 \quad (3.6)$$

$$O_3^{-\bullet} + H^+ \rightarrow HO_3^{\bullet} \quad (3.7)$$

$$HO_3^{\bullet} \rightarrow O_2 + {}^{\bullet}OH \quad (3.8)$$

Ozone, which is formed by the well known reaction of atomic oxygen with molecular oxygen, is a selective oxidant which reacts at somewhat different rates with the three forms of SMZ described above, the second order rate constant (k_{O3}) being equal to $3.3{\cdot}10^5$, $4.7{\cdot}10^5$ and $5.7{\cdot}10^5$ $M^{-1}{\cdot}s^{-1}$ for the protonated, neutral and anionic forms, respectively (Qiang et al., 2004; Dodd et al., 2006). As for the OH radical, the second order rate constant for its reaction with SMZ was determined to be $(7.63 \pm 0.85){\cdot}10^9$ $M^{-1}{\cdot}s^{-1}$ within the 3–8 pH range, suggesting that the reactivities of the neutral and anionic forms of SMZ are very similar (Yang et al., 2017). These data show first of all that, expectedly, the rate constant for reaction with OH radicals is always way larger than that for reaction with ozone (*ca* 10^4 times larger). This does not mean at all that reaction with ozone in our reactor is negligible, because the rate of reaction with

ozone is proportional to the product k_{O3}·[O_3] and, although k_{O3} is 10^4 times lower than k_{OH}, the concentration of ozone is much higher than that of the OH radical. Indeed, the important contribution of ozone to advanced oxidation of organic pollutants in the DBD plasma reactor used here was highlighted and discussed in a recent paper reporting on the reaction of maleic and fumaric acid (Shapoval et al., 2023). Another important conclusion drawn from the kinetic data for oxidation of SMZ found in the literature and cited above is that its neutral and ionized species react with similar rates. Therefore, the speciation of SMZ is not the major contribution to the dependence of SMZ degradation rate on pH observed in this study, dependence which is thus attributed mainly to the pH-dependent availability of the reactive species involved, OH radicals and ozone. Notably, more OH radicals are expected to form in neutral/basic solutions than in acidic solutions due to more efficient ozone degradation (Staehelin and Hoigné, 1982). These conclusions are consistent with those of a recent study which reports on and discusses the pH dependence of the steady state concentration of OH radicals in this reactor (Tomei et al., 2023). Moreover, a similar pH effect was reported recently for SMZ degradation by a falling water film DBD plasma/persulfate system (Shang et al., 2022). An opposite trend was instead observed in SMZ degradation induced by a DBD plasma jet (Hu et al., 2023) in solutions (not buffered) with initial pH values of 3.0, 5.4, 7.0 and 10.3, the fastest kinetics being recorded in acidic solutions. The rationale offered by the Authors to explain the rate reduction observed in basic solution is that OH radicals are quenched by hydroxide ions to form water and atomic oxygen radical ion. Additionally, the Authors also note that in acidic solutions (pH 3–5) SMZ is present in its neutral form which has a higher mass transfer coefficient than the anionic form, thus increasing the degradation rate (Hu et al., 2023).

Similarly to our conclusions, Hu et al. (Hu, 2023) also identify OH radicals and ozone as the main reactive species responsible for the initial attack on SMZ. Both the rate of OH radical production and the ozone concentrations reported by Hu et al. for DBD discharge in pure oxygen are higher than those achieved by the DBD discharge in air used in this work. Specifically, their rate of OH radical production is more than three times higher than ours, $2.1 \cdot 10^{-8}$ M·s^{-1} and $0.63 \cdot 10^{-8}$ M·s^{-1} (Marotta et al., 2011), respectively. As for ozone, while the amount dissolved in water was below detection limit in our reactor using air as plasma feed gas, it reached 1 mg/L in 8 min in theirs using oxygen as plasma feed gas. These data are fully consistent and explain the higher rate of SMZ degradation and mineralization obtained by Hu et al. than reported here. While use of pure oxygen instead of air and recirculation of the gas and of the treated water have obvious advantages, there are additional costs implied which will have to be considered in scaling-up operations.

As for the energy efficiency of the process, under best operating conditions, a G_{50} value of 6.4 g/kWh was achieved in this study, which is in line with the majority of values reported for analogous treatments in various non-thermal plasma set-ups which were recently reviewed (Bilea et al., 2024). As mentioned before, we worked at constant power aiming at maintaining stable and reproducible discharge conditions which are necessary for reliable kinetic studies. Thus, we made no attempts in this work to optimize the set-up, discharge and reactor, which are certainly viable for improvement. Notably, a considerably better result than our was obtained in treating SMZ (50 mg/L initial concentration) in a DBD reactor of different design using air as plasma feed gas and achieving a G_{50} value of 47.6 g/kWh, estimated from their data in Figure 2B (Kim et al., 2015). As in many NTP set-ups, use of oxygen instead of air brings about great improvements in kinetics and energy efficiency in this DBD driven process (Kim et al., 2015). An additional increment in efficiency is achieved by recirculating both the gas and the solution and by mixing them in an external ozonation unit thus taking better advantage of the ozone produced by the discharge (Hu et al., 2023; Bilea et al., 2024).

3.2 Transformation products and mineralization

Mineralization of a complex organic molecule proceeds via numerous steps and involves many oxidation intermediates and byproducts. The transformation products and the mechanisms leading to SMZ mineralization in nature and in various advanced oxidation processes including NTP have been extensively investigated and the results of these studies form a useful basis to interpret the results reported here. It is known that hydroxylation, cleavage of S-N bond, oxidation of the amino group, oxidation of the methyl group, oxidation of the C-C double bond in the isoxazole ring, and isomerization are the main pathways of SMZ degradation under most AOPs conditions (Gómez-Ramos et al., 2011; Liu et al., 2012; Kim et al., 2015; Shahidi et al., 2015; Peleyeju et al., 2017; Prasannamedha and Senthil Kumar, 2020; Shang et al., 2022; Hu et al., 2023; Bilea et al., 2024). Transformation products may be toxic and persist after the total removal of the parent compound. It is therefore important to identify them and characterize their reactivity under the conditions used for the treatment. Coupled analyses by HPLC-UV/Vis and LC-MS/MS allowed us to identify several transformation products during SMZ degradation in our DBD plasma reactor. Although these products were not quantified, based on peak areas it was found that their global amount at any stage of the treatment was a marginal fraction of the total organic carbon originally present as SMZ. Interestingly, the same products were detected under all the experimental conditions tested (pH 2, pH 7 and pH 11).

The powerful diagnostic capabilities of MS^2 analysis were exploited to characterize the transformation products detected at various reaction times during SMZ treatment in our DBD reactor. To start with, the MS^2 spectrum of sulfamethoxazole itself is reported (Figure 3A) and briefly described (Scheme 1) since it can be very useful in interpreting the MS^2 spectra of its transformation products and therefore in identifying them. Support for the interpretation of our results is provided by an interesting study on the preferred protonation site of SMZ in the gas phase under ESI conditions similar to those used in our work (Uhlemann et al., 2021). It was found that, in contrast with protonation in acidic aqueous media which occurs at the aromatic primary amino group, under positive ESI ionization conditions the favored protonation site is the nitrogen atom included in the heterocycle. As seen in Figure 3A, protonated SMZ dissociates to give as most abundant fragment ion a species with m/z 156, which was previously identified as the sulfanilyl

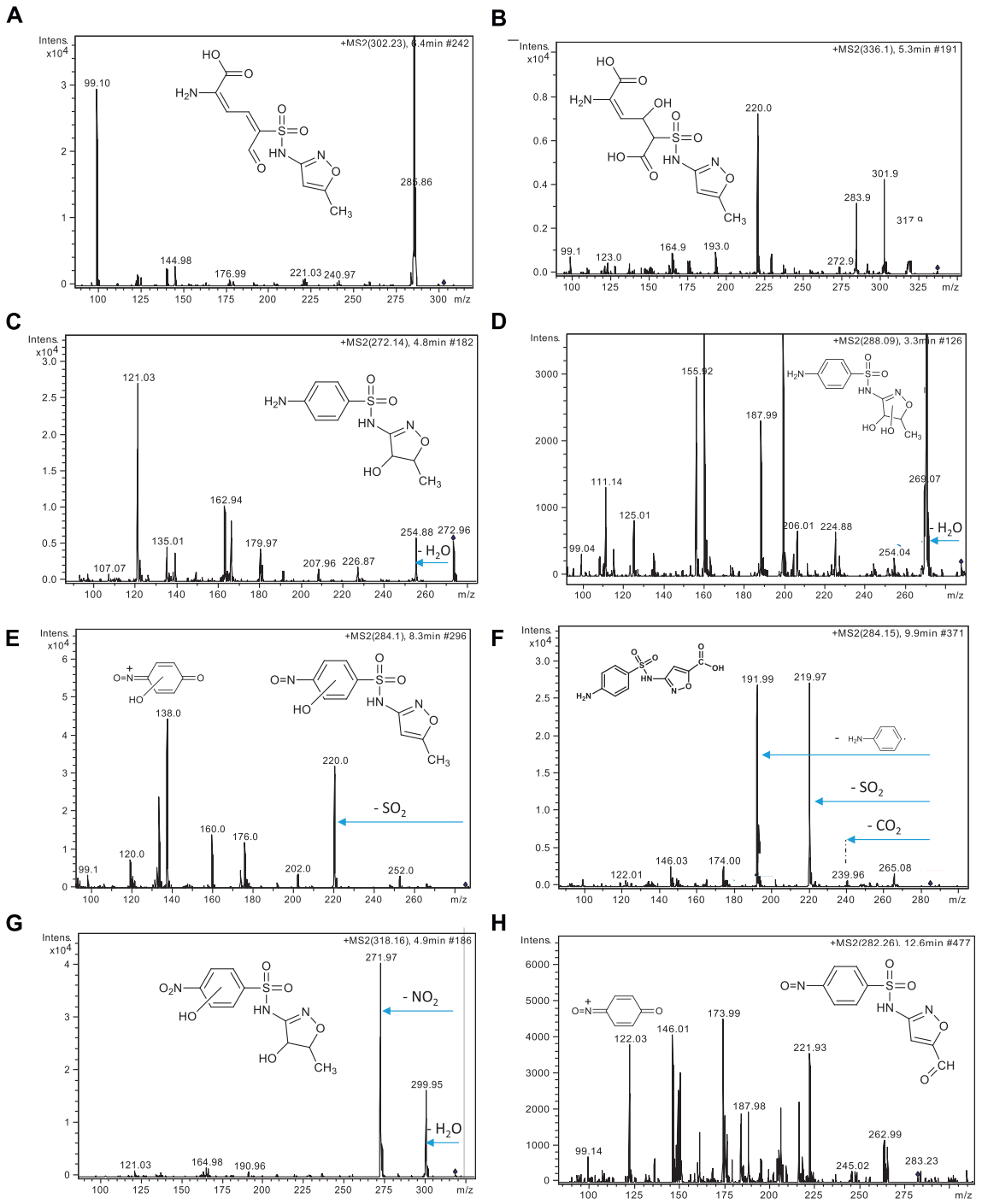

FIGURE 2
MS^2 spectra of some intermediates of SMZ degradation detected at **(A)** m/z 302, **(B)** m/z 336, **(C)** m/z 272, **(D)** m/z 288, **(E)** and **(F)** m/z 284, **(G)** m/z 318 and **(H)** m/z 282.

fragment, $H_2N–C_6H_4–SO_2^+$, a highly stabilized ion due to charge delocalization (Uhlemann et al., 2021), as shown in Scheme 1.

Associated with the para-amino sulfonyl moiety of SMZ are also the two signals at m/z 108 and 92 which are attributed to ionic fragments $[H_2N\text{-}C_6H_4\text{-}O]^+$ and $[H_2N\text{-}C_6H_4]^+$, respectively. Another diagnostically important signal is that at m/z 99, which is assigned to protonated 3-amino-5-methylisoxazole and is likewise useful as the m/z 156 signal discussed above in the analysis and interpretation of the spectra of SMZ transformation products. The two provide complementary structural information. Thus, the presence of either of these two signals, m/z 99 or m/z 156 in the MS^2 spectrum of a transformation product allowed us to identify which part of the SMZ structure had undergone oxidative attack, the para-amino-benzene ring or the isoxazole ring, respectively.

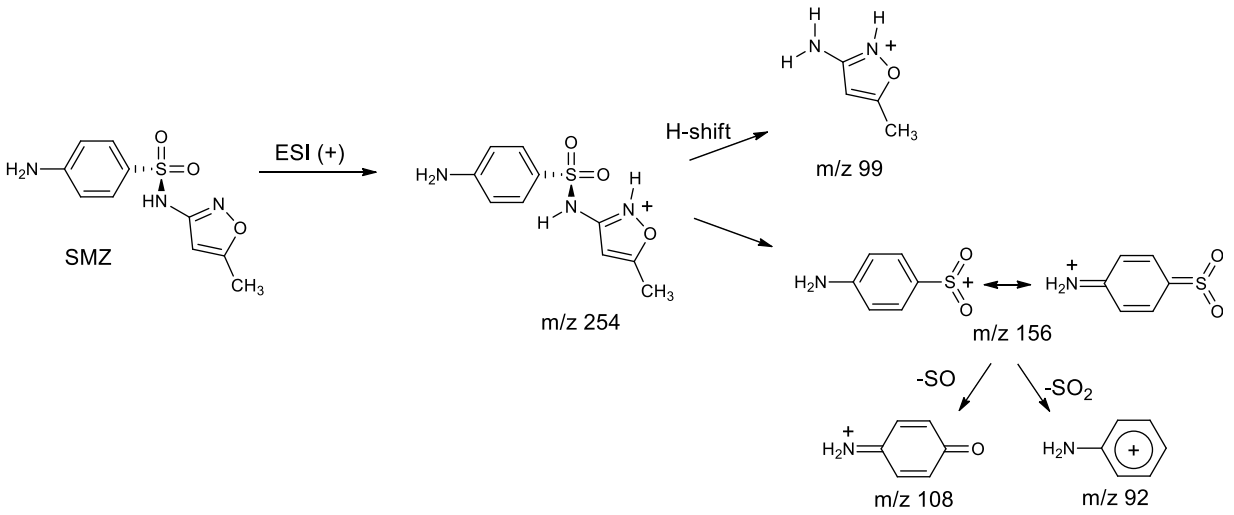

SCHEME 1
Main fragmentation pathway of protonated SMZ in the MS^2 spectrum.

Among the transformation products observed by coupled HPLC-UV/Vis and LC-MS/MS analyses of SMZ plasma treated solution, the most abundant was 3-amino-5-methylisoxazole (P-99, m/z 99) (Figure 3B). This product, due to cleavage of the S-N sulfonamide bond, has been observed in various types of SMZ advanced oxidation and is also reported to be its major product of degradation in the aqueous environment. In nature, S-N bond rupture can occur via direct photolysis or via indirect photolysis, initiated primarily by attack of OH radicals on the benzene ring at the carbon atom linked to sulfur (Ge et al., 2018). Specifically, the S-N bond dissociation energy is significantly lower than of that of alternative sites of cleavage in SMZ, including the C-S and the N-$C_{isoxazole}$ bonds (Wu et al., 2024). Interestingly, the product of S-N bond cleavage, 3-amino-5-methylisoxazole, is not among the 38 transformation products detected in SMZ treatment by a combined non-thermal plasma-ozonation process described recently in the literature (Bilea et al., 2024). Similarly, Hu and coworkers, who searched for this product, failed to detect it in their study of SMZ degradation by DBD plasma and concluded that probably it is too reactive, under the conditions tested, to accumulate in sufficient amounts to be detected (Hu et al., 2023). Additional transformation products detected in our analyses include two compounds with m/z 270 (Figures 3B, C), attributed to products formed by hydroxylation of SMZ in two different positions. Thanks to MS/MS analysis, it was possible to characterize their structures: the presence of the ionic fragments at m/z 156, 108 and 92 (Figure 3C), detected also in the fragmentation of SMZ (Figure 2A), suggests that in this isomer, the para-aminophenyl mojety linked to the sulphoxide group is not modified and that hydroxylation has occurred on the isoxazole ring. In the mass spectrum of the other isomer (Figure 3D), the ionic fragment at m/z 156 is not present, indicating that attack of ·OH has instead occurred on the benzene ring. This hypothesis is supported by the presence in the mass spectrum of the signal at m/z 99, typical of the isoxazole ring, which therefore has been preserved intact in this product. Furthermore, substitution of the amino group by the hydroxyl group leads to the formation of a dihydroxylated product at m/z 271 (P-271) (Figure 3E).

Transformation products originating from the reaction of SMZ with ozone were also detected: the products at m/z 302 (Figure 2A), 320 (not shown) and 336 (Figure 2B) originate from addition of ozone to the para-amino benzene ring and breakdown of the resulting ozonide (von Sonntag and von Gunten, 2012), followed, in the case of products at m/z 336 and m/z 320, by addition of a water molecule. Addition of a water molecule on SMZ, which is supposed to take place on the isoxazole ring, produces a compound at m/z 272 (Figure 2C), while the same reaction on the product with m/z 270 generates P-288 (Figure 2D) (Kim et al., 2015), a dihyroxylated sulfamethoxazole, which shows a fragmentation pattern similar to that of SMZ including the tracer signals at m/z 108 and m/z 156.

Another interesting finding was the identification of two isomeric compounds with m/z 284 but different elution times (Figures 2E, F). These products can be differentiated based on their fragmentation patterns and comparison with data reported in the literature (Gómez-Ramos et al., 2011). Specifically, the spectrum shown in Figure 2E matches that reported in the literature for the product in which oxidation has occurred in the para-amino benzene mojety of SMZ as shown in the figure. The second isomer P-284 (Figure 2F) was instead identified as the product of oxidation of the isoxazolic methyl group to the corresponding carboxylic acid, showing the characteristic loss of 44 u (-CO_2), typical fragmentation of carboxylic acids. The two major fragmentation signals seen at m/z 220 and m/z 192 (Figure 2F) are consistent with the proposed structure for this isomer, resulting from SO_2 elimination (and rearrangement) and C-S bond rupture, respectively. No traces of the product with -NH_2 oxidized to -NO_2 with m/z 284 was detected in our analyses, even though this product was reported among the primary products in SMZ ozonation (Gómez-Ramos et al., 2011). However, a transformation product with m/z 318 shows the loss of 46 u, attributed to–NO_2, indicating a product in which -NH_2 was

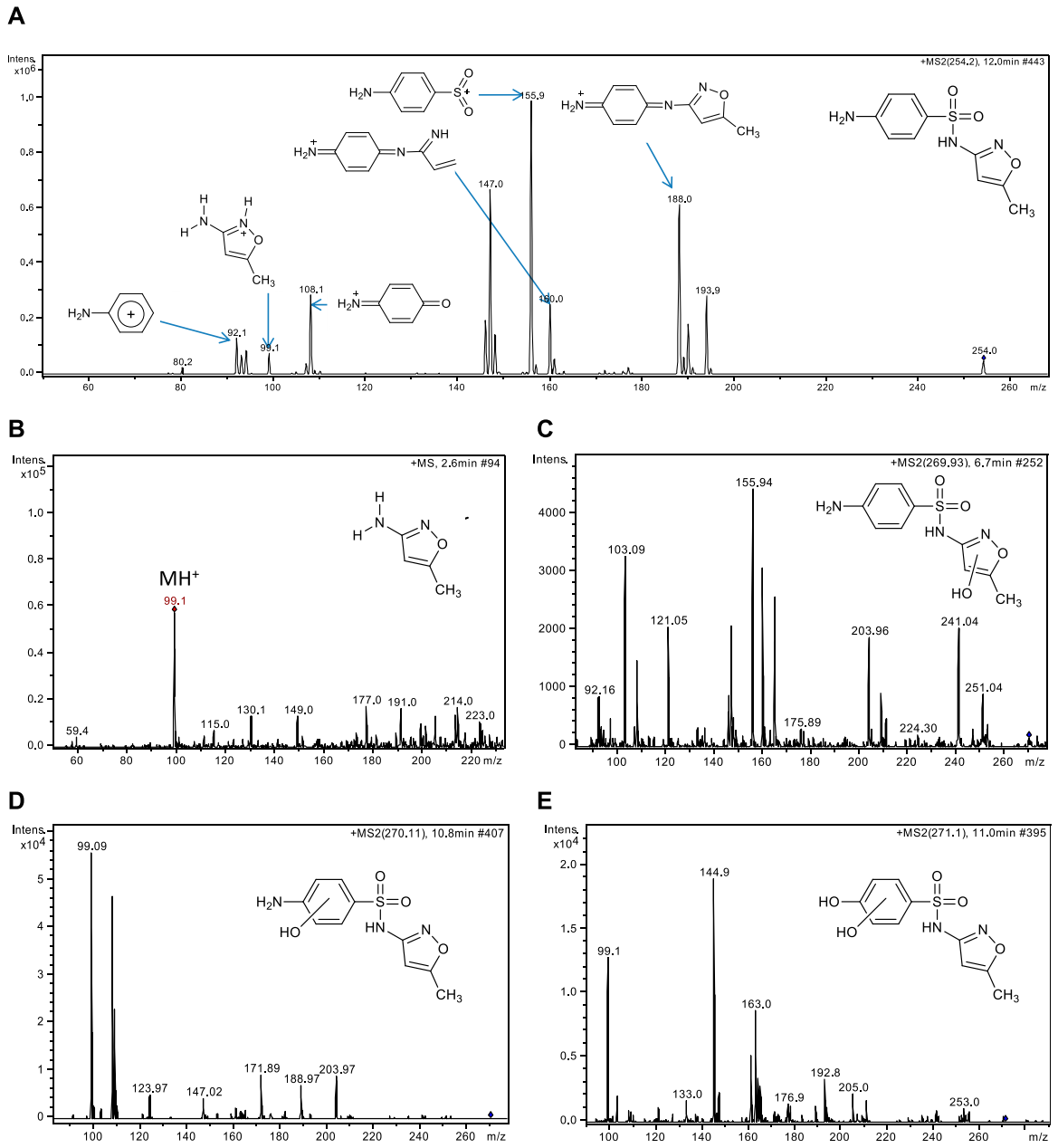

FIGURE 3
MS, MS^2 spectra and structures of SMZ and of some transformation products of plasma treatment: **(A)** MS^2 spectrum of SMZ, **(B)** MS spectrum of the most abundant transformation product of SMZ oxidation at m/z 99, **(C)** and **(D)** MS^2 spectra of two isomeric transformation products detected at m/z 270 and **(E)** product at m/z 271.

oxidized to -NO_2 but characterized also by hydroxylation of the benzene ring and addition of a water molecule on the isoxazole ring (Figure 2G). Finally, a hypothesis is formulated for the structure of a product detected at m/z 282 (Figure 2H), in which oxidation of both the methyl group in the isoxazole ring to a formyl group and of the amino group of the benzene ring to -NO has occurred. The MS/MS spectrum is not easy to be interpreted, but the proposed structure is reasonable and consistent with the fragment observed at m/z 122, attributed to the ion drawn in the figure.

In conclusion, degradation of SMZ in our plasma reactor proceeds via transformation products which have been mostly identified previously along major degradation pathways under various AOP conditions, including NTP (Kim et al., 2015; Hu et al., 2023; Bilea et al., 2024). All can be traced to the action of OH radicals and ozone, which were determined previously as major oxidants in the DBD reactor used in this study (Marotta et al., 2011; Krishna et al., 2016; Shapoval et al., 2023; Tomei et al., 2023).

As mentioned before, the solution pH affects both the speciation of SMZ and the distribution and amounts of the reactive species. Indeed, it was found earlier that the degradation pathways of SMZ are also affected by the solution pH (Dodd et al., 2006; Gómez-Ramos et al., 2011; Hu et al., 2023). It was therefore of interest to

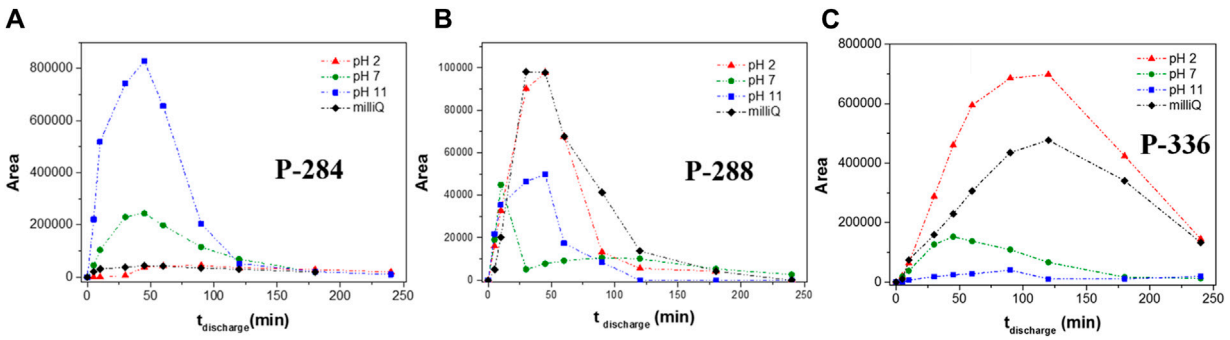

FIGURE 4
UV-HPLC areas of **(A)** P-284, **(B)** P-288 and **(C)** P-336 as a function of treatment time.

investigate the product distribution obtained in our plasma treatment carried out under various pH conditions. As an example, we show and discuss here the pH dependence of three transformation products, the hydroxylated product with m/z 284 and two products, with m/z 336 and m/z 288, respectively, in which addition of a water molecule has occurred to the isoxazole C-C double bond.

Figure 4 describes the changes of the chromatographic peak areas, which are proportional to the product abundances, as a function of treatment time, recorded in experiments carried out under different pH conditions. It can be noted that for transformation products with m/z 288 and m/z 336, larger areas are obtained under acidic than under basic pH, while the opposite trend is observed for P-284. These findings are fully consistent with the known conditions favoring the reactions proposed for the formation of these products. Specifically, with regard to hydroxylated product P-284 (Figure 4A), it is known that hydroxyl radical attack on the benzene ring is promoted at pH > 7, when the formation of ·OH is favored and the amino group is not protonated. On the contrary, addition of a water molecule to the C-C double bond of the isoxazole ring is favored under acidic pH conditions, accounting for the observed pH dependence of products P-288 and P-336 shown in Figures 4B, C, respectively. It is important to note that, although these transformation products are affected in different ways by the solution pH, efficient decomposition of all of them was achieved under neutral pH conditions, leading to their complete removal.

Finally, the extent of mineralization was also investigated, considering that the ultimate goal in water remediation is the exhaustive degradation of any organic pollutants into CO_2. Production of CO_2 from the oxidation of sulfamethoxazole in our process was confirmed by qualitative FT-IR analysis of the air flowing out of the plasma reactor. To quantify the extent of mineralization, total carbon was measured in solution before and after plasma treatment, using a SMZ solution with $8{\cdot}10^{-6}$ M initial concentration. We chose this concentration, which is indeed unrealistically high, significantly higher than that found in the worst-case scenario of poultry wastewater treatment (Asha and Kumar, 2015), because it was suitable to guarantee reliable quantitative determinations. Treatment of this solution in our plasma reactor achieved complete mineralization in 6 h, a remarkable result considering the modest mineralization rates generally observed for SMZ under most AOPs conditions, including those of typical NTP based processes. Exceptions are a Fe^{2+}-montmorillonite catalyzed ozonation process in which total mineralization of SMZ was obtained (Shahidi et al., 2015) and the recent results of He et al. (2024), who identified bacteria strains able to metabolize SMZ and achieving 98% of SMZ mineralization. On the contrary, to the best of our knowledge, this is the first report of SMZ complete mineralization obtained by NTP. Thus, most studies employing NTP and NTP plus catalysts report only partial, and often quite limited, mineralization extent achieved in treatments which last typically no longer than a few tens of minutes, a duration sufficient to completely degrade SMZ and its major detected transformation products, but way too short to achieve exhaustive mineralization. Long treatment times, as we report here, are obviously uneconomical and impractical. However, considering the dependence of degradation kinetics on the pollutant concentration described earlier (the lower the concentration the faster the process), it is expected that mineralization times will be shorter for treatment of SMZ at concentrations which are lower and more realistic than used in this experiment. Moreover, as mentioned earlier, our target in designing this plasma reactor was to obtain stable and reproducible discharge conditions needed for kinetic studies and there is ample opportunity to optimize its efficiency. Notably, the best result published so far is probably the remarkable SMZ mineralization extent of 90% obtained in 20 min using a DBD plasma jet reactor with oxygen as plasma feed gas and with recycling of both gas and solution (Hu et al., 2023) to take advantage of the ozone produced by the discharge.

3.3 Toxicity assessment

The evaluation of SMZ solutions ($5{\cdot}10^{-4}$ M) toxicity before and after plasma treatment (4 h) is of interest because oxidation products could be as toxic or even more toxic than their precursor contaminant. Several case studies described a toxicity increase as a consequence of the oxidation of organic contaminants in water (Zazo et al., 2005; Huang et al., 2015; Hübner et al., 2015). The battery of selected toxicity tests (i.e., *A. fischeri, R. subcapitata,* and *D. magna*) was used previously to investigate the effects of other AOP technologies (Gómez-Ramos et al., 2011; Gong and Chu, 2016; Cardito et al., 2024; Morante et al., 2024; Rescigno et al.,

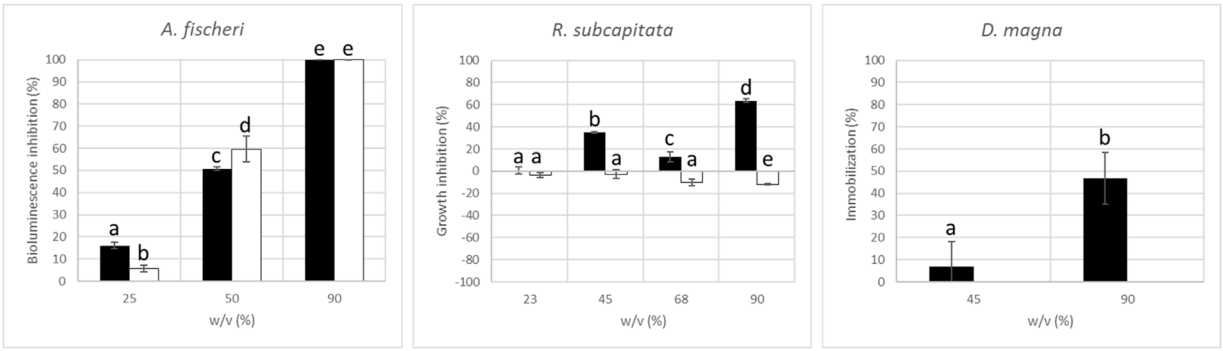

FIGURE 5
Results of wastewater/volume ratio (w/v) obtained in the toxicity tests of *A. fischeri* bioluminescence inhibition (30 min), *R. subcapitata* growth inhibition (72 h), and *D. magna* mortality (48 h); data with different letters (a–e) are significantly different (Tukey's, $p < 0.05$) within the same picture; error bars represent standard deviations ($n = 3$).

TABLE 3 Toxicity results expressed according to Persoone et al. (2003).

Samples	*A. fischeri*		*R. subcapitata*		*D. magna*		*Final score*
	% Effect	Score	% Effect	Score	% Effect	Score	
Untreated $5{\cdot}10^{-4}$ M SMZ solution	100	2	64	2	47	1	*1.7*
4 h—treated SMZ solution	100	2	−12	0	0	0	*0.7*

2024). In the case of NTP treatments of SMZ-contaminated solutions, most papers evaluate the toxicity of the treated water considering the toxicity of the detected transformation products predicted by the ECOSAR program (Shang et al., 2022; Hu et al., 2023; Bilea et al., 2024). Based on this approach, transformation products turned out to be more, equally or less toxic than SMZ depending on their structure, so the estimation of the final toxicity of the solution requires a detailed description of its chemical composition. Moreover, there can be an increase or the preservation of the solution toxicity after a short treatment times and a progressive toxicity decrease as the mineralization degree increases with the increase of the treatment time. Similar trends are effectively found by Hu et al. (2023) on *E. coli* and by Lee et al. (2018) using *Daphnia magna*.

At first, we carried out control experiments using plasma-treated ultrapure water and obtained not significant effects. According to Figure 5, EC50 values can be determined only for *A. fischeri*: before treatment (50.6 ± 4.3)%; after treatment (51.4 ± 3.6)% with no significantly different effects ($\alpha = 0.05$) before and after treatment. Conversely, microalgae and daphnids suggested a complete removal of SMZ and any other toxic transformation products after 4 h of plasma treatment. In particular, *R. subcapitata* showed biostimulation at the highest exposure concentrations (90%) after treatment suggesting that by-products from SMZ can promote algal growth. Indeed, SO_4^{2-}, $N\text{-}NH_4^+$ and $N\text{-}NO_3^-$ ions, in addition to inorganic carbon and carbon sources released by the organic contaminant, may serve as nutrient for algae growth. $N\text{-}NH_4^+$ can be also formed during plasma treatment and its detection was already reported in the literature for plasma [9] and other AOPs [35]. Moreover, $N\text{-}NO_3^-$ are produced by air non-thermal plasma in water.

According to Persoone et al. (2003) as summarized in Table 3, the treatment administered to samples reduced the toxicity from acute (before treatment) to slightly acute (after treatment).

These results suggested the importance of an ecotoxicological characterization of AOP treated samples carried out experimentally and involving different categories of organisms. Indeed, even at very low concentrations, organic pollutants escaping from the wastewater treatment may potentially impair the ecosystem.

4 Conclusion

Remarkable results were achieved in the treatment of SMZ-contaminated water using a previously described simple benchtop reactor in which air non-thermal plasma is generated above the liquid by DBD discharges. Indicators used to assess the process performance include the rate of SMZ degradation, the types and time evolution of transformation products, the extent of mineralization, i.e., of total organic carbon removed as CO_2, the process energy efficiency and the quality of the treated polluted water as assessed by well-established toxicological assays. Specifically, the results highlight that, if complete mineralization is not obtained, it is important to verify the ecotoxicological compatibility of the treated water with different categories of organisms before its reuse or final discharge in surface water bodies. Evidently, any toxic transformation products formed en route to mineralization are likewise or more reactive than SMZ

under the adopted experimental conditions used in this work and therefore do not accumulate. This conclusion is supported by the results of experimentally determined concentration vs. treatment time profiles for the main transformation products which were detected by LC/MS and identified by MS^2 analyses. Small numbers and amounts of transformation products are strong and most desirable features of the described process. Based on previous findings concerning AOPs activated by air plasma in the reactor used in this work and on literature data about SMZ oxidation mechanisms and products, it is concluded that the observed transformation products are formed in SMZ reactions initiated by either the OH radical or ozone. The simple set-up used in this study was by no means optimized and is amenable to improvements to achieve faster kinetics and higher energy yields, as well as, in perspective, also to scaling up. Envisioned implementations include gas and solution recycling, as reported in the literature (Hu et al., 2023; Bilea et al., 2024), in order to take full advantage of ozone and of its reaction with hydrogen peroxide, both of which are produced by the discharge, as well as coupling with a green power source to make the energy requirement sustainable.

Data availability statement

The raw data supporting the conclusion of this article will be made available by the authors, without undue reservation.

Author contributions

AG: Data curation, Investigation, Writing–original draft. GL: Writing–original draft, Methodology. GL: Data curation, Writing–review and editing. AS: Data curation, Investigation, Writing–original draft. EM: Funding acquisition, Supervision, Writing–review and editing. CP: Resources, Supervision, Writing–review and editing.

Funding

The author(s) declare that financial support was received for the research, authorship, and/or publication of this article. We acknowledge financial support under the National Recovery and Resilience Plan (PNRR), Mission 4, Component 2, Investment 1.1, Call for tender No. 104 published on 2.2.2022 by the Italian Ministry of University and Research (MUR), funded by the European Union–NextGenerationEU–Project Title "Cyanotoxins oxidation by atmospheric plasma, a green technology for water decontamination–PLASMADETOX"–CUP C53D23004460006–Grant Assignment Decree No. 1064 adopted on 18 July 2023 by the Italian Ministry of Ministry of University and Research (MUR). Open Access funding provided by Università degli Studi di Padova | University of Padua, Open Science Committee.

Acknowledgments

The stimulating environment provided by COST Action 19110 is gratefully acknowledged.

Conflict of interest

The authors declare that the research was conducted in the absence of any commercial or financial relationships that could be construed as a potential conflict of interest.

Publisher's note

References

Aggelopoulos, C. A. (2022). Recent advances of cold plasma technology for water and soil remediation: a critical review. *Chem. Eng. J.* 428, 131657. doi:10.1016/j.cej.2021.131657

Andreozzi, R., Raffaele, M., and Nicklas, P. (2003). Pharmaceuticals in STP effluents and their solar photodegradation in aquatic environment. *Chemosphere* 50, 1319–1330. doi:10.1016/S0045-6535(02)00769-5

Ang, W. L., McHugh, P. J., and Symes, M. D. (2022). Sonoelectrochemical processes for the degradation of persistent organic pollutants. *Chem. Eng. J.* 444, 136573. doi:10.1016/j.cej.2022.136573

Asha, R. C., and Kumar, M. (2015). Sulfamethoxazole in poultry wastewater: identification, treatability and degradation pathway determination in a membrane-photocatalytic slurry reactor. *J. Environ. Sci. Health A* 50, 1011–1019. doi:10.1080/10934529.2015.1038161

Bilea, F., Bradu, C., Cicirma, M., Medvedovici, A. V., and Magureanu, M. (2024). Plasma treatment of sulfamethoxazole contaminated water: intermediate products, toxicity assessment and potential agricultural reuse. *Sci. Tot. Environ.* 90920, 168524. doi:10.1016/j.scitotenv.2023.168524

Biondo, O., Tomei, G., Saleem, M., Sretenović, G. B., Magarotto, M., Marotta, E., et al. (2023). Products, reactive species and mechanisms of PFOA degradation in a self-pulsing discharge (SPD) plasma reactor. *Chemosphere* 341, 139972. doi:10.1016/j.chemosphere.2023.139972

Bosi, F. J., Tampieri, F., Marotta, E., Bertani, R., Pavarin, D., and Paradisi, C. (2017). Characterization and comparative evaluation of two atmospheric plasma sources for water treatment. *Plasma process. Polym.* 15, 1700130. doi:10.1002/ppap.201700130

Bruggeman, P. J., Kushner, M. J., Locke, B. R., Gardeniers, J. G. E., Graham, W. G., Graves, D. B., et al. (2016). Plasma–liquid interactions: a review and roadmap. *Plasma Sources Sci. Technol.* 25, 053002. doi:10.1088/0963-0252/25/5/053002

Cardito, A., Carotenuto, M., Sacco, O., Albarano, L., Vaiano, V., Iannece, P., et al. (2024). UV light assisted degradation of acid orange azo dye by ZVI-ZnS and effluent toxicity effects. *Environ. Pollut.* 343, 123226. doi:10.1016/j.envpol.2023.123226

Ceriani, E., Marotta, E., Schiorlin, M., Ren, X., Ceretta, C., Gobbo, R., et al. (2018b). A versatile prototype plasma reactor for water treatment supporting different discharge regimes. *J. Phys. D. Appl. Phys.* 51, 274001. doi:10.1088/1361-6463/aac7cd

Ceriani, E., Marotta, E., Shapoval, V., Favaro, G., and Paradisi, C. (2018a). Complete mineralization of organic pollutants in water by treatment with air non-thermal plasma. *Chem. Eng. J.* 337, 567–575. doi:10.1016/j.cej.2017.12.107

Dodd, M. C., Buffle, M. O., and von Gunten, U. (2006). Oxidation of antibacterial molecules by aqueous ozone: moiety-specific reaction kinetics and application to ozone-based wastewater treatment. *Environ. Sci. Technol.* 40, 1969–1977. doi:10.1021/es051369x

EU (2022). Commission Implementing Decision (EU) 2022/1307 of 22 July 2022 establishing a watch list of substances for Union-wide monitoring in the field

of water policy pursuant to Directive 2008/105/EC of the European Parliament and of the Council (2022). *Off. J. Eur. Union L* 197, 117–121.

Foster, J. E. (2017). Plasma-based water purification: challenges and prospects for the future. *Phys. Plasma.* 24, 055501. doi:10.1063/1.4977921

Ge, P., Yu, H., Chen, J., Qu, J., and Luo, Y. (2018). Photolysis mechanism of sulfonamide moiety in five-membered sulfonamides: a DFT study. *Chemosphere* 197 (2018), 569–575. doi:10.1016/j.chemosphere.2018.01.041

Giardina, A., Tampieri, F., Biondo, O., Marotta, E., and Paradisi, C. (2019). Air non-thermal plasma treatment of the herbicides mesotrione and metolachlor in water. *Chem. Eng. J.* 372, 171–180. doi:10.1016/j.cej.2019.04.098

Giardina, A., Tampieri, F., Marotta, E., and Paradisi, C. (2018). Air non-thermal plasma treatment of Irgarol 1051 deposited on TiO2. *Chemosphere* 210, 653–661. doi:10.1016/j.chemosphere.2018.07.012

Gómez-Ramos, M. delM., Mezcua, M., Agüera, A., Fernández-Alba, A. R., Gonzalo, S., Rodríguez, A., et al. (2011). Chemical and toxicological evolution of the antibiotic sulfamethoxazole under ozone treatment in water solution. *J. Hazard. Mater.* 192, 18–25. doi:10.1016/j.jhazmat.2011.04.072

Gong, H., and Chu, W. (2016). Determination and toxicity evaluation of the generated products in sulfamethoxazole degradation by UV/CoFe2O4/TiO2. *J. Hazard. Mater.* 314, 197–203. doi:10.1016/j.jhazmat.2016.04.052

Guo, H., Su, Y., Yang, X., Wang, Y., Li, Z., Wu, Y., et al. (2023). Dielectric barrier discharge plasma coupled with catalysis for organic wastewater treatment: a review. *Catalysts* 13, 10. doi:10.3390/catal13010010

He, Y., Liu, L., Wang, Q., Dong, X., Huang, J., Jia, X., et al. (2024). Bio-degraded of sulfamethoxazole by microbial consortia without addition nutrients: mineralization, nitrogen removal, and proteomic characterization. *J. Hazard. Mater.* 466, 133558. doi:10.1016/j.jhazmat.2024.133558

Hu, S., Yan, W., Yu, J., Zhu, B., Lan, Y., Xi, W., et al. (2023). Degradation of sulfamethoxazole in water by dielectric barrier discharge plasma jet: influencing parameters, degradation pathway, toxicity evaluation. *Plasma Sci. Technol.* 25, 035510. doi:10.1088/2058-6272/ac9d85

Huang, H., Liu, G., Lv, W., Yao, K., Kang, Y., Li, F., et al. (2015). Ozone-oxidation products of ibuprofen and toxicity analysis in simulated drinking water. *J. Drug Metab. Toxicol.* 6, 1000181. doi:10.4172/2157-7609.1000181

Hübner, U., von Gunten, U., and Jekel, M. (2015). Evaluation of the persistence of transformation products from ozonation of trace organic compounds-A critical review. *Water Res.* 68, 150–170. doi:10.1016/j.watres.2014.09.051

ISO (1998). *Water quality: determination of the inhibitory effect of water samples on the light emission of Vibrio fischeri (Luminescent bacteria test). Part 3: method using freeze-dried bacteria*. Geneva: ISO.

ISO (2012). *Water quality– fresh water algal growth inhibition test with unicellular green Algae.8692*. Geneva: ISO.

ISO (2013). *Water quality: determination of the inhibition of the mobility of Daphnia magna straus (cladocera, Crustacea) – acute toxicity test*. Geneva: ISO.

Jiang, B., Zheng, J., Qiu, S., Wu, M., Zhang, Q., Yan, Z., et al. (2014). Review on electrical discharge plasma technology for wastewater remediation. *Chem. Eng. J.* 236, 348–368. doi:10.1016/j.cej.2013.09.090

Kim, K., Kam, S. K., and Mok, Y. S. (2015). Elucidation of the degradation pathways of sulfonamide antibiotics in a dielectric barrier discharge plasma system. *Chem. Eng. J.* 271, 31–42. doi:10.1016/j.cej.2015.02.073

Krishna, S., Ceriani, E., Marotta, E., Giardina, A., Špatenka, P., and Paradisi, C. (2016). Products and mechanism of verapamil removal in water by air non-thermal plasma treatment. *Chem. Eng. J.* 292, 35–41. doi:10.1016/j.cej.2016.01.108

Lee, J.-C., Nam, J.-Y., and Kim, H.-W. (2018). Degradation of sulfonamide antibiotics and their intermediates toxicity in an aeration-assisted non-thermal plasma while treating strong wastewater. *Chemosphere* 209, 901–907. doi:10.1016/j.chemosphere.2018.06.125

Libralato, G., Volpi Ghirardini, A., and Avezzù, F. (2010). How toxic is toxic? A proposal for wastewater toxicity hazard assessment. *Ecotoxicol. Environ. Saf.* 73, 1602–1611. doi:10.1016/j.ecoenv.2010.03.007

Liu, X., Garoma, T., Chen, Z., Wang, L., and Wu, Y. (2012). SMX degradation by ozonation and UV radiation: a kinetic study. *Chemosphere* 87, 1134–1140. doi:10.1016/j.chemosphere.2012.02.007

Lofrano, G., Libralato, G., Adinolfi, R., Siciliano, A., Iannece, P., Guida, M., et al. (2016). Photocatalytic degradation of the antibiotic chloramphenicol and effluent toxicity effects. *Ecotoxicol. Environ. Saf.* 123, 65–71. doi:10.1016/j.ecoenv.2015.07.039

Madureira, J., Ceriani, E., Pinhão, N., Marotta, E., Melo, R., Cabo Verde, S., et al. (2017). Oxidation of clofibric acid in aqueous solution using a non-thermal plasma discharge or gamma radiation. *Chemosphere* 187, 395–403. doi:10.1016/j.chemosphere.2017.08.109

Magureanu, M., Bilea, F., Bradu, C., and Hong, D. (2021). A review on non-thermal plasma treatment of water contaminated with antibiotics. *J. Hazard. Mater.* 417, 125481. doi:10.1016/j.jhazmat.2021.125481

Magureanu, M., Mandache, N. B., and Parvulescu, V. I. (2015). Degradation of pharmaceutical compounds in water by non-thermal plasma treatment. *Water Res.* 81, 124–136. doi:10.1016/j.watres.2015.05.037

Manzo, R. H., and de Bertorello, M. M. (1973). Isoxazoles I: protonation of isoxazole derivatives in aqueous sulfuric acid. *J. Pharm. Sci.* 62, 152–154. doi:10.1002/jps.2600620136

Marotta, E., Callea, A., Ren, X., Rea, M., and Paradisi, C. (2008). DC corona electric discharges for air pollution control, 2—ionic intermediates and mechanisms of hydrocarbon processing. *Plasma process. Polym.* 5, 146–154. doi:10.1002/ppap.200700128

Marotta, E., Ceriani, E., Schiorlin, M., Ceretta, C., and Paradisi, C. (2012). Comparison of the rates of phenol advanced oxidation in deionized and tap water within a dielectric barrier discharge reactor. *Water Res.* 46, 6239–6246. doi:10.1016/j.watres.2012.08.022

Marotta, E., Schiorlin, M., Ren, X., Rea, M., and Paradisi, C. (2011). Advanced oxidation process for degradation of aqueous phenol in a dielectric barrier discharge reactor. *Plasma process. Polym.* 8, 867–875. doi:10.1002/ppap.201100036

Morante, N., Tammaro, O., Albarano, L., De Guglielmo, L., Oliva, N., Sacco, O., et al. (2024). Influence of visible light LEDs modulation techniques on photocatalytic degradation of ceftriaxone in a flat plate reactor. *Chem. Eng. J.* 482, 149175. doi:10.1016/j.cej.2024.149175

Morin-Crini, N., Lichtfouse, E., Fourmentin, M., Ribeiro, A. R. L., Noutsopoulos, C., Mapelli, F., et al. (2022). Removal of emerging contaminants from wastewater using advanced treatments. A review. *Environ. Chem. Lett.* 20, 1333–1375. doi:10.1007/s10311-021-01379-5

Mouele, M. E. S., Myint Myo, T. Z., Kyaw, H. H., Tijani, J. O., Dinu, M., Parau, A. C., et al. (2022). Degradation of sulfamethoxazole by double cylindrical dielectric barrier discharge system combined with Ti/C-N-TiO2 supported nanocatalyst. *J. Hazard Mater. Adv.* 5, 100051. doi:10.1016/j.hazadv.2022.100051

Naghdi, S., Shahrestani, M. M., Zendehbad, M., Djahaniani, H., Kazemian, H., and Eder, D. (2023). Recent advances in application of metal-organic frameworks (MOFs) as adsorbent and catalyst in removal of persistent organic pollutants (POPs). *J. Hazard. Mater.* 442, 130127. doi:10.1016/j.jhazmat.2022.130127

Oberoi, A. S., Jia, Y., Zhang, H., Khanal, S. K., and Lu, H. (2019). Insights into the fate and removal of antibiotics in engineered biological treatment systems: a critical review. *Environ. Sci. Technol.* 53 (13), 7234–7264. doi:10.1021/acs.est.9b01131

Peleyeju, M. G., Umukoro, E. H., Tshwenya, L., Moutloali, R., Babalola, J. O., and Arotiba, O. A. (2017). Photoelectrocatalytic water treatment systems: degradation, kinetics and intermediate products studies of sulfamethoxazole on a TiO2-exfoliated graphite electrode. *RSC Adv.* 7, 40571–40580. doi:10.1039/c7ra07399b

Persoone, G., Marsalek, B., Blinova, I., Törökne, A., Zarina, D., Manusadzianas, L., et al. (2003). A practical and user-friendly toxicity classification system with microbiotests for natural waters and wastewaters. *Environ. Toxicol.* 18, 395–402. doi:10.1002/tox.10141

Prasannamedha, G., and Senthil Kumar, P. (2020). A review on contamination and removal of sulfamethoxazole from aqueous solution using cleaner techniques: present and future perspective. *J. Clean. Prod.* 250, 119553. doi:10.1016/j.jclepro.2019.119553

Qiang, Z., Adams, C., and Surampalli, R. (2004). Determination of ozonation rate constants for lincomycin and spectinomycin. *Ozone Sci. Eng.* 26, 525–537. doi:10.1080/01919510490885334

Qiao, J., and Xiong, Y. (2021). Electrochemical oxidation technology: a review of its application in high-efficiency treatment of wastewater containing persistent organic pollutants. *J. Water Process Eng.* 44, 102308. doi:10.1016/j.jwpe.2021.102308

Rescigno, R., Sacco, O., Pragliola, S., Albarano, L., Libralato, G., Lofrano, G., et al. (2024). Environmentally safe ZVI/ZnS-based polymer composite for lindane degradation in water: assessment of photocatalytic activity and eco-toxicity. *Sep. Purif. Technol.* 330, 125246. doi:10.1016/j.seppur.2023.125246

Shahidi, D., Moheb, A., Abbas, R., Larouk, S., Roy, R., and Azzouz, A. (2015). Total mineralization of sulfamethoxazole and aromatic pollutants through Fe2+-montmorillonite catalyzed ozonation. *J. Hazard. Mater.* 298, 338–350. doi:10.1016/j.jhazmat.2015.05.029

Shang, K., Li, J., and Morent, R. (2019). Hybrid electric discharge plasma technologies for water decontamination: a short review. *Plasma Sci. Technol.* 21, 043001. doi:10.1088/2058-6272/aafbc6

Shang, K., Morent, R., Wang, N., Wang, Y., Peng, B., Jiang, N., et al. (2022). Degradation of sulfamethoxazole (SMX) by water falling film DBD plasma/persulfate: reactive species identification and their role in SMX degradation. *Chem. Eng. J.* 431, 133916. doi:10.1016/j.cej.2021.133916

Shapoval, V., Ceriani, E., Frezzato, D., Paradisi, C., and Marotta, E. (2023). Plasma treatment and ozonation of binary mixtures: the case of maleic and fumaric acids. *Plasma Chem. Plasma process.* 43, 1709–1729. doi:10.1007/s11090-023-10399-8

Staehelin, J., and Hoigné, J. (1982). Decomposition of ozone in water: rate of initiation by hydroxide ions and hydrogen peroxide. *Environ. Sci. Technol.* 16, 676–681. doi:10.1021/es00104a009

Subramaniam, M. N., Goh, P. S., Kanakaraju, D., Lim, J. W., Lau, W. J., and Ismail, A. F. (2022). Photocatalytic membranes: a new perspective for persistent organic pollutants removal. *Environ. Sci. Pollut. Res.* 29, 12506–12530. doi:10.1007/s11356-021-14676-x

Takeuchi, N., and Yasuoka, K. (2021). Review of plasma-based water treatment technologies for the decomposition of persistent organic compounds. *Jpn. J. Appl. Phys.* 60, SA0801. doi:10.35848/1347-4065/abb75d

Tampieri, F., Durighello, A., Biondo, O., Gąsior, M., Knyś, A., Marotta, E., et al. (2019). Kinetics and products of air plasma induced oxidation in water of imidacloprid and thiamethoxam treated individually and in mixture. *Plasma Chem. Plasma process.* 39, 545–559. doi:10.1007/s11090-019-09960-1

Tomei, G., Saleem, M., Ceriani, E., Pinton, A., Marotta, E., and Paradisi, C. (2023). Cold plasma for green advanced reduction/oxidation processes (AROPs) of organic pollutants in water. *Chem. Eur. J.* 29, e202302090. doi:10.1002/chem.202302090

Uhlemann, T., Berden, G., and Oomens, J. (2021). Preferred protonation site of a series of sulfa drugs in the gas phase revealed by IR spectroscopy. *Eur. Phys. J. D.* 75, 23. doi:10.1140/epjd/s10053-020-00027-x

Vanraes, P., Nikiforov, A. Y., and Leys, C. (2016). "Electrical discharge in water treatment technology for micropoulltant decomposition," in *Plasma science and technology - progress in physical states and chemical reactions*. Editor T. Mieno (London: IntechOpen Limited), 428–478. doi:10.5772/61830

von Sonntag, C., and von Gunten, U. (2012). *Chemistry of ozone in water and wastewater treatment: from basic principles to applications*. London: Iwa Publishing.

Wang, J., and Wang, S. (2018). Microbial degradation of sulfamethoxazole in the environment. *Appl. Microbiol. Biotechnol.* 102, 3573–3582. doi:10.1007/s00253-018-8845-4

Wang, Y., Huang, J., Guo, H., Puyang, C., Han, J., Li, Y., et al. (2022). Mechanism and process of sulfamethoxazole decomposition with persulfate activated by pulse dielectric barrier discharge plasma. *Sep. Purif. Technol.* 287, 120540. doi:10.1016/j.seppur.2022.120540

Wu, L., Wang, M., Rong, L., Wang, W., Chen, L., Wu, Q., et al. (2024). Structural effects of sulfonamides on the proliferation dynamics of sulfonamide resistance genes in the sequencing batch reactors and the mechanism. *J. Environ. Sci.* 135, 161–173. doi:10.1016/j.jes.2022.11.014

Yang, Y., Lu, X., Jiang, J., Ma, J., Liu, G., Cao, Y., et al. (2017). Degradation of sulfamethoxazole by UV, UV/H2O2 and UV/persulfate (PDS): formation of oxidation products and effect of bicarbonate. *Water Res.* 118, 196–207. doi:10.1016/j.watres.2017.03.054

Zazo, J. A., Casas, J. A., Mohedano, A. F., Gilarranz, M. A., and Rodriguez, J. J. (2005). Chemical pathway and kinetics of phenol oxidation by fenton's reagent. *Environ. Sci. Technol.* 39, 9295–9302. doi:10.1021/es050452h

Zhang, H., Xiao, S., Du, Y., Song, S., Hu, K., Huang, Y., et al. (2022). Catalysis of MnO2-cellulose acetate composite films in DBD plasma system and sulfamethoxazole degradation by the synergistic effect. *Sep. Purif. Technol.* 298, 121608. doi:10.1016/j.seppur.2022.121608